

Tunable chiral symmetry breaking in symmetric Weyl materials

Sahal Kaushik,^{1,*} Evan John Philip,^{1,2,†} and Jennifer Cano^{1,3,‡}

¹*Department of Physics and Astronomy, Stony Brook University, Stony Brook, NY 11794, USA*

²*Computational Science Initiative, Brookhaven National Laboratory, Upton, NY 11973, USA*

³*Center for Computational Quantum Physics, Flatiron Institute, New York, NY 10010, USA*

Asymmetric Weyl semimetals, which possess an inherently chiral structure, have different energies and dispersion relations for left- and right-handed fermions. They exhibit certain effects not found in symmetric Weyl semimetals, such as the quantized circular photogalvanic effect and the helical magnetic effect. In this work, we derive the conditions required for breaking chiral symmetry by applying an external field in symmetric Weyl semimetals. We explicitly demonstrate that in certain materials with the T_d point group, magnetic fields along low symmetry directions break the symmetry between left- and right-handed fermions; the symmetry breaking can be tuned by changing the direction and magnitude of the magnetic field. In some cases, we find an imbalance between the number of type I left- and right-handed Weyl cones (which is compensated by the number of type II cones of each chirality.)

I. INTRODUCTION

Dirac [1–10] and Weyl [11–18] semimetals have linear and gapless dispersion relations, forming effective low-energy massless fermions (see Ref. [19] for a review). They exhibit interesting effects such as the chiral magnetic effect [20] and negative longitudinal magnetoresistance [18, 21–28].

Massless fermions have a well-defined chirality given by the sign of the product of momentum and (pseudo)spin. Dirac semimetals have doubly degenerate bands, with fermions of both chiralities at the same place in the Brillouin zone; their band crossings are not topologically protected, but can be symmetry protected [6]. In contrast, in Weyl semimetals, fermions of different chiralities are separated in momentum space. Consequently, Weyl semimetals exhibit some chirality-dependent effects not found in Dirac semimetals, such as a photocurrent induced by circularly polarized light [29, 30], and elliptically polarized terahertz emission in response to pulsed circularly polarized near infrared light [31].

Certain phenomena require the left- and right-handed fermions to have different energies or velocities. They include the quantized circular photogalvanic effect [32], the helical magnetic effect [33] and the chiral magnetic effect without a source of chirality [34]. These effects are possible only in materials that have chiral crystal lattices which lack non-orientation-preserving symmetries. We refer to such materials as asymmetric Weyl materials, and materials that do have orientation-reversing symmetries as symmetric Weyl materials. Asymmetric Weyl materials include RhSi[35] and CoSi[36]. The quantized circular photogalvanic effect has been observed in both these materials [37, 38].

However, asymmetric Weyl materials are rare in nature compared to symmetric Weyl materials. In this work, we

show that a symmetric Weyl material can be turned into an asymmetric one by applying an external field that breaks all non-orientation-preserving symmetries. We study this phenomenon in a family of zincblende materials and derive several quantities that measure the chirality breaking. We then explicitly show that in the zincblende material InAs, applying a magnetic field in a low symmetry direction breaks all non-orientation-preserving symmetries, and causes left- and right-handed fermions to have different velocities and energies. This induced asymmetry allows for the observation of effects present only in asymmetric Weyl materials. As a byproduct, we show examples where the number of type I Weyl fermions [39] of left- and right-chirality are not equal; the imbalance is compensated by the number of type II Weyl fermions of each chirality.

II. PROPERTIES OF WEYL CONES

The chirality of a Weyl fermion is $\chi = \text{sgn}(\vec{s} \cdot \vec{p})$ where \vec{s} is the pseudospin and \vec{p} is the momentum. The chirality is positive for right-handed fermions and negative for left-handed fermions. Since Weyl cones are monopoles of Berry curvature and the total Berry charge in the Brillouin zone must be zero, there is always an equal number of left- and right-handed Weyl cones in a microscopic Hamiltonian.

Under inversion symmetry (P), the pseudospin, momentum, and chirality transform as

$$\begin{aligned}\vec{s} &\rightarrow \vec{s} \\ \vec{p} &\rightarrow -\vec{p} \\ \chi &\rightarrow -\chi\end{aligned}\tag{1}$$

Under time-reversal symmetry (T), the pseudospin, momentum, and chirality transform as

$$\begin{aligned}\vec{s} &\rightarrow -\vec{s} \\ \vec{p} &\rightarrow -\vec{p} \\ \chi &\rightarrow \chi\end{aligned}\tag{2}$$

* sahal.kaushik@stonybrook.edu

† ephilip@bnl.gov

‡ jennifer.cano@stonybrook.edu

In a material that has both inversion and time-reversal symmetries, the chirality flips under P and remains invariant under T . Crystal momentum k_i flips sign under both P and T . Therefore, under PT ,

$$\begin{aligned} k_i &\rightarrow k_i \\ \chi &\rightarrow -\chi \end{aligned} \quad (3)$$

In such a material, the left- and right-handed fermions coincide in the Brillouin zone; thus, it has Dirac cones, not Weyl cones. Therefore, all Weyl materials lack time-reversal, inversion or both.

Non-orientation-preserving symmetries transform left-handed fermions into right-handed fermion and vice versa. Therefore, in materials with these symmetries, each left-handed cone has a right-handed partner cone at the same energy and with the same velocities. Consequently, effects such as the quantized circular photogalvanic effect, which requires an asymmetry between left- and right-handed cones, are possible only in materials that have a chiral crystal lattice without orientation-reversing symmetries.

The cones of Weyl fermions are generally tilted. Fermions with small tilts and elliptical Fermi surfaces are called type I Weyl fermions, while those with large tilts and hyperbolic Fermi surfaces are called type II Weyl fermions [39]. A sketch of the dispersion relations of type I and type II Weyl cones is shown in Figure 1. Many Weyl semimetals have exclusively type I fermions, such as TaAs [15–17, 40]. Some materials have only type II fermions, such as WTe₂ [41]. The Weyl semimetal OsC₂ is unusual in that it has both kinds of Weyl cones—24 of type I and 12 of type II [42].

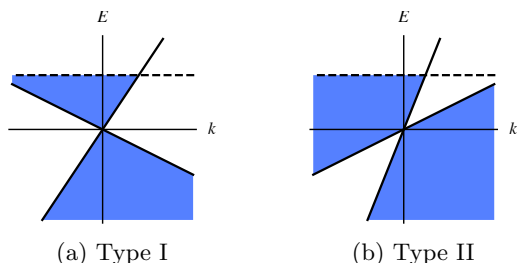


FIG. 1: Dispersion relations of type I and type II tilted Weyl cones. The dashed line shows the Fermi level. Blue shading indicates the filled Fermi sea.

The linearized Hamiltonian for a general Weyl cone is

$$H = v_t^i q_i + v_a^i \sigma_a q_i + E, \quad (4)$$

where v_t^i is the “tilt” velocity and v_a^i represents the untilted part of the Hamiltonian. E is the energy of the Weyl point. The matrices σ_a act on spin or pseudospin. The chirality is

$$\chi = \text{sgn}(\det(v_a^i)), \quad (5)$$

which is positive for a right-handed cone and negative for a left-handed cone. We define the product of velocities

$$v_1 v_2 v_3 = |\det(v_a^i)|, \quad (6)$$

the velocity tensor $(v_W^2)^{ij} = v_a^i v_a^j$ and its inverse $(v_W^{-2})_{ij}$. We also define a dimensionless measure of the tilt

$$\text{tilt parameter} = \sqrt{(v_W^{-2})_{ij} v_t^i v_t^j}. \quad (7)$$

The cone is type I if the tilt parameter is less than 1 and type II if it is greater than 1 [39].

III. TRUE AND FALSE CHIRALITY

L. D. Barron introduced the idea of true and false chirality of a system [43]. A Weyl material is said to have false chirality if it possesses a symmetry MT , where M is some non-orientation-preserving symmetry, but does not have the symmetry M itself. Such a material transforms to its mirror image under time reversal. Systems with true chirality retain their chirality even under time reversal. Examples of systems with true chirality include glucose and DNA molecules and the electroweak part of the Standard Model. Systems with false chirality include a cone rotating about its axis and a crystal with inversion symmetry subjected to parallel uniform electric and magnetic fields.

Asymmetric Weyl materials, such as RhSi and CoSi, have crystal structures with true chirality. Materials with false chirality cannot be asymmetric Weyl materials, because the chirality of each cone is invariant under T but flips under M (since, by definition, M reverses orientation), so left- and right-handed cones would be related by MT .

In symmetric Weyl materials, it is possible to break mirror symmetries by applying external perturbations. Such symmetry breaking may produce either true or false chirality, as we will demonstrate. As a first example, consider the transition metal monpnitride class of materials, which includes TaAs, TaP, NbAs, and NbP [14–17, 40, 44–46]. These compounds have tetragonal symmetry and are in the space group $I4_1md$ (No. 109) with fourfold rotation about the [001] axis, reflection symmetry about the [100], [010], [110], $[\bar{1}10]$ planes, and time-reversal symmetry, but no inversion symmetry or reflection symmetry about the [001] plane. If we apply a magnetic field along the [001] direction, B_z flips sign under reflections and therefore breaks all mirror symmetries. However, this perturbation does not introduce true chirality as B_z also flips sign under time-reversal; therefore the perturbed system remains invariant under symmetries MT , where M is a mirror reflection symmetry of the unperturbed system. Thus, TaAs with a magnetic field along the c axis has false chirality and would therefore still be a symmetric Weyl material.

Only systems with true chirality will display effects that depend on a difference in energy or velocity between

left- and right-handed fermions. Such effects will correspond to the expectation value of an operator, Q , such that Q is invariant under all orientation-preserving symmetries of the unperturbed system, but flips sign under all non-orientation-preserving symmetries. For a perturbation λ to produce true chirality in the system, there must exist a function $Q(\lambda)$ with this property.

For systems that possess time-reversal symmetry, a quantity that is of odd order in magnetic field does not qualify as $Q(\lambda)$ because it is odd under time-reversal, which preserves chirality. For example, in the transition metal monpnictides mentioned above, B_z is invariant under rotation, and flips under reflections, but since it also flips under time-reversal, which preserves the chiralities of fermions, operators that are odd in B_z will yield a vanishing expectation value. The lowest order function of \vec{B} that transforms in the same way as the chirality of fermions under all symmetries of the unperturbed system is $Q(\vec{B}) = B_x B_y (B_x^2 - B_y^2)$. Similarly, if we consider chirality induced by strain along a low symmetry axis, the lowest order $Q(S)$ is $S_{xy}(S_{xx} - S_{yy})$. Therefore, in TaAs, we expect physical phenomena such as the helical magnetic effect to be of fourth order in \vec{B} or second order in S_{ij} . The effects of a low symmetry perturbation are illustrated in Figure 2.

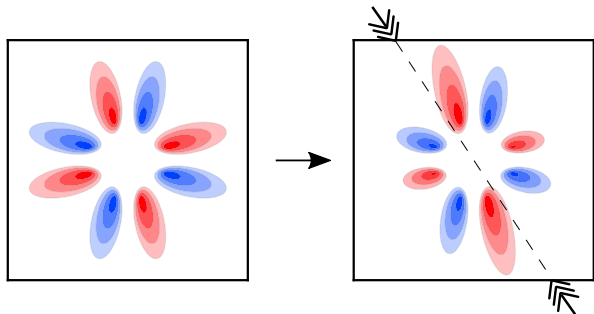


FIG. 2: Slices of the Fermi surface for a Weyl material with fourfold rotation symmetry such as TaAs. The shading represents energy and the color represents chirality of the fermions. Each ellipse represents a Weyl cone. A perturbation along a low symmetry axis, such as a strain or a magnetic field, would affect left- and right-handed cones differently, resulting in a net chiral asymmetry.

In materials that possess inversion symmetry, external magnetic fields or uniform strain cannot induce chirality, because both magnetic field and strain are even under parity, and any functions of these quantities will also be even under parity. Since most Dirac materials such as ZrTe_5 and Na_3Bi have inversion symmetry, we cannot transform them into asymmetric Weyl materials through uniform strain or uniform external magnetic field. However, it is possible to create symmetric Weyl cones and other topological phases in materials such as ZrTe_5 with Zeeman splitting [47].

In this work, we focus on a class of non-

centrosymmetric materials that have the space group $F43m$ (No. 216) and the point group T_d . This class includes the half-Heusler compound GdPtBi [48] and the zincblende compounds HgTe and InSb . These materials have several axes of rotation and planes of reflection, as well as time-reversal symmetry, but they lack inversion symmetry. Their electronic structure is characterized by a fourfold degeneracy at the Γ point and no Weyl cones. However, if we apply an external magnetic field [49] or strain [50], or if there is magnetic ordering [48, 51], the degeneracy splits, and Weyl points appear. When the degeneracy is broken by a magnetic field along high symmetry axes, such as [111] and [100], all the emergent Weyl fermions come in pairs of opposite chirality related by symmetry [49]. In the next section, we will show that this is not the case when the magnetic field is along a low-symmetry axis.

IV. MODEL

We consider the Hamiltonian given in Ref. [49]:

$$\begin{aligned}
 H = AI_4 + C \left[(k_x^2 - k_y^2)\Gamma_1 + \frac{1}{\sqrt{3}}(2k_z^2 - k_x^2 - k_y^2)\Gamma_2 \right] \\
 + E(k_x k_y \Gamma_3 + k_x k_z \Gamma_4 + k_y k_z \Gamma_5) \\
 + D(k_x U_x + k_y U_y + k_z U_z) \\
 + \mu_B g (B_x J_x + B_y J_y + J_z B_z), \quad (8)
 \end{aligned}$$

where $J_{x,y,z}$ are the spin- $\frac{3}{2}$ matrices, which can be expressed as

$$J_x = \begin{pmatrix} 0 & \frac{\sqrt{3}}{2} & 0 & 0 \\ \frac{\sqrt{3}}{2} & 0 & 1 & 0 \\ 0 & 1 & 0 & \frac{\sqrt{3}}{2} \\ 0 & 0 & \frac{\sqrt{3}}{2} & 0 \end{pmatrix}, \quad (9)$$

$$J_y = \begin{pmatrix} 0 & -\frac{i\sqrt{3}}{2} & 0 & 0 \\ \frac{i\sqrt{3}}{2} & 0 & -i & 0 \\ 0 & i & 0 & -\frac{i\sqrt{3}}{2} \\ 0 & 0 & \frac{i\sqrt{3}}{2} & 0 \end{pmatrix}, \quad (10)$$

$$J_z = \begin{pmatrix} \frac{3}{2} & 0 & 0 & 0 \\ 0 & \frac{1}{2} & 0 & 0 \\ 0 & 0 & -\frac{1}{2} & 0 \\ 0 & 0 & 0 & -\frac{3}{2} \end{pmatrix} \quad (11)$$

The matrices Γ_μ are defined as

$$\begin{aligned}
 \Gamma_1 &= \frac{1}{\sqrt{3}}(J_x^2 - J_y^2) \\
 \Gamma_2 &= \frac{1}{3}(2J_z^2 - J_x^2 - J_y^2) \\
 \Gamma_3 &= \frac{1}{\sqrt{3}}\{J_x, J_y\} \\
 \Gamma_4 &= \frac{1}{\sqrt{3}}\{J_x, J_z\} \\
 \Gamma_5 &= \frac{1}{\sqrt{3}}\{J_y, J_z\}
 \end{aligned} \quad (12)$$

These matrices satisfy the anticommutation relations $\{\Gamma_\mu, \Gamma_\nu\} = 2\delta_{\mu\nu}$. The matrices U_i are defined as

$$\begin{aligned} U_x &= \frac{1}{2i}(\sqrt{3}[\Gamma_1, \Gamma_5] - [\Gamma_2, \Gamma_5]) \\ U_y &= \frac{-1}{2i}(\sqrt{3}[\Gamma_1, \Gamma_4] + [\Gamma_2, \Gamma_4]) \\ U_z &= \frac{1}{i}[\Gamma_2, \Gamma_3] \end{aligned} \quad (13)$$

The unperturbed Hamiltonian (at zero magnetic field) has time-reversal and T_d symmetry. The coefficient D represents an inversion breaking term.

We seek an expression $Q(\vec{B})$ that indicates true chirality. As discussed in the previous section, $Q(\vec{B})$ must be even(odd) under symmetries that maintain(reverse) the chirality of a Weyl cone. The expression $B_x B_y B_z$ represents false chirality because it is odd under time-reversal and even under $S_4 T$, where S_4 is the rotoinversion symmetry about the z axis that maps $(x, y, z) \mapsto (y, -x, -z)$. The lowest order polynomial of B that represents a true chirality breaking term is $Q(\vec{B}) = (B_x^2 - B_y^2)(B_y^2 - B_z^2)(B_z^2 - B_x^2)$. It is non-zero only when the magnetic field is away from high symmetry axes such as [100], [110], and [111]. In what follows, we will use the dimensionless quantity

$$Q'(\hat{B}) = (B_x^2 - B_y^2)(B_y^2 - B_z^2)(B_z^2 - B_x^2)/B^6 \quad (14)$$

as a measure of chirality breaking. $Q'(\hat{B})$ takes a maximum value of 0.0962 when $\hat{B} = (0, 0.460, 0.888)$ or points in a symmetry-related direction.

The Hamiltonian defined by equation (8) is a lowest order expansion in k that is only valid for a finite range of crystal momentum and energy; at higher energies, mixing with other bands becomes important. Therefore, when we search for Weyl points in this Hamiltonian with an applied magnetic field, we choose a cut-off in crystal momentum and energy and only focus on Weyl points that are within this cutoff. We ensure that the cutoff always contains the same number of left- and right-handed Weyl points.

We will now focus on the zincblende material InSb. It has six bands closest to the Fermi level, consisting of a set of four valence bands that meet at Γ very close to $E = 0$ and a set of two conduction bands separated by a bandgap of 235 meV. The set of four is modeled by the Hamiltonian in equation (8) with parameters as given in Table I [49, 52–54].

V. WEYL FERMIONS IN INDIUM ANTIMONIDE IN A MAGNETIC FIELD

When a magnetic field is applied along a general low-symmetry direction, the induced Weyl points are not related to each other by any symmetry. There is no analytical expression for their positions and each one must

A	$8.85 \text{ eV}\text{\AA}^2$
C	$14.2 \text{ eV}\text{\AA}^2$
D	$0.01 \text{ eV}\text{\AA}$
E	$-22 \text{ eV}\text{\AA}^2$
g -factor	51

TABLE I: Hamiltonian parameters in Eq. (8) corresponding to InSb.

be located numerically by diagonalizing Eq. (8). We will search for Weyl points within the cutoffs $k < 0.032 \text{\AA}^{-1}$ and $E < 50 \text{ meV}$. For all magnitudes and directions of magnetic field considered in our work, there is an equal number of left- and right-handed Weyl cones within these cutoffs.

In addition to $Q'(\hat{B})$, we characterize the chirality breaking by a dimensionless parameter

$$\delta_v = \sum \chi v_1 v_2 v_3 / \sum v_1 v_2 v_3, \quad (15)$$

where the product of velocities $v_1 v_2 v_3$ is defined in (6) and the sum is over all the cones. We also define a dimensionful chirality breaking parameter

$$\delta_E = \sum \chi E / n \quad (16)$$

where n is the total number of right-handed Weyl cones (equal to the total number of left-handed Weyl cones). Physically, δ_v represents the average difference in velocities of the left- and right-handed Weyl cones normalized by the average velocity, while δ_E represents the average difference in energy between left- and right-handed Weyl cones. While $Q'(\hat{B})$ serves as a quick check to determine which low-symmetry directions are likely to have the largest chirality breaking, δ_v and δ_E are directly related to known physical observables [32–34]. Note that $Q'(\hat{B}) \neq 0$ is a necessary condition for the left- and right-handed cones to have different energies and velocities, and thus for δ_v , δ_E , and relevant physical observables to be non-zero.

In Table II, we have listed the energy, momentum, chirality, velocity and tilt of all ten Weyl cones that appear for a magnetic field of 0.75 T along the low symmetry direction [147]. The chirality breaking parameter $Q'(\hat{B})$ for this direction is 0.0826, close to the maximum possible value of 0.0962. For this field, we observe three type I Weyl cones and seven type II Weyl cones: unexpectedly, the type I (or type II) Weyl cones do not come in pairs of opposite chirality, which is only possible in asymmetric Weyl materials.

In Table III, we have listed the number of type I and type II cones of each chirality, and the chirality breaking parameters δ_v and δ_E , for different magnitudes of magnetic field along the [147] direction. Table III shows that δ_v , the dimensionless average velocity difference between left- and right-handed Weyl cones, increases with increasing magnitude of the magnetic field, even while

$Q'(\hat{B})$ remains constant. The average energy difference, δ_E , also increases with increasing field. Thus, we expect physical observables that depend on a difference in energy or velocity between Weyl cones will increase as the magnetic field is increased along this direction.

The same quantities are recorded in Table IV for different directions of magnetic field and fixed magnitude 0.75 T. Here the three measures of chirality-breaking, $Q'(\hat{B})$, δ_v and δ_E can be compared: δ_v and δ_E show similar trends as $Q'(\hat{B})$, but are not functions of $Q'(\hat{B})$. Because of the complexities of the band structure and topology, they do not even necessarily vary monotonically with $Q'(\hat{B})$: they can change sign or even be zero for some low-symmetry directions of \vec{B} . Both Tables III and IV show that it is not unusual to find different numbers of left- and right-handed Weyl cones of the same type in this model.

As an example, the positions of cones of different types and chiralities for a magnetic field of 0.75 T along the directions [001], [111], and [147] are shown in Figure 3.

k_x	k_y	k_z	χ	Energy	Bands	$v_1 v_2 v_3$	Tilt	Type
(10^8 m^{-1})				(meV)		$(\text{eV}^3 \text{ pm}^3)$		
-0.229	-0.569	0.782	L	-1.36	1-2	5830	0.706	I
-0.755	-0.572	-0.802	L	1.82	2-3	13200	1.19	II
0.812	-0.432	-0.782	L	1.32	2-3	9350	1.20	II
-0.083	-0.302	1.093	L	0.20	2-3	1780	1.87	II
-2.114	-0.120	-0.304	L	11.72	3-4	12.6	333	II
-0.016	-0.579	1.058	R	0.10	2-3	2950	0.585	I
0.310	0.462	-0.733	R	-1.59	1-2	4390	0.710	I
0.735	0.533	0.837	R	1.81	2-3	11400	1.32	II
-0.762	0.344	0.865	R	1.30	2-3	6430	1.57	II
-1.648	-0.335	-0.119	R	7.45	3-4	44.7	40.1	II

TABLE II: Weyl cones for a magnetic field of 0.75T along the low symmetry direction [147]. The first three columns specify the crystal momentum of the Weyl point; the next columns indicate its chirality; its energy; the two bands that comprise it, where band 1 has the lowest energy; its product of velocities; its tilt; and whether it is type 1 or type II. The chirality χ , product of velocities $v_1 v_2 v_3$ and tilt are defined in Eqs. (5), (6), and (7), respectively.

VI. OUTLOOK

Asymmetric Weyl materials are sought-after to observe chirality-breaking effects such as the quantized circular photogalvanic effect [32], the helical magnetic effect [33], and the chiral magnetic effect without an external source of chirality [34]. Yet few of these materials have been shown to exist naturally. Therefore, in this work, we proposed inducing an asymmetry between the left- and right-handed Weyl cones in otherwise symmetric materials by an applied field, such as strain or magnetic field,

B	Type I		Type II		δ_v	δ_E
(T)	Left	Right	Left	Right	(meV)	
0.500	1	2	4	3	-0.0820	-0.39
0.625	1	2	4	3	-0.0863	-0.64
0.750	1	2	4	3	-0.0907	-0.92
0.875	1	2	4	3	-0.0953	-1.25
1.000	1	1	4	4	-0.1012	-1.61

TABLE III: Number of left- and right-handed cones of each type, and chirality breaking parameters for variable magnetic field B along the low symmetry direction [147]. The chirality breaking parameters δ_v and δ_E are defined by Eq. (15) and Eq. (16) respectively.

Dir	$Q'(\hat{B})$	Type I		Type II		δ_v	δ_E
		Left	Right	Left	Right	(meV)	
[111]	0	5	5	0	0	0	0
[345]	0.00806	2	3	2	1	0.00042	0.0034
[123]	0.0437	1	2	4	3	-0.0175	-0.26
[147]	0.0826	1	2	4	3	-0.0907	-0.92
[001]	0	3	3	0	0	0	0

TABLE IV: Number of left- and right-handed cones of each type and chirality breaking parameters for magnetic field of magnitude 0.75 T along different directions (Dir). The chirality breaking parameters Q' , δ_v and δ_E are defined by Eq. (14), Eq. (15) and Eq. (16) respectively.

along a low-symmetry direction. We have also provided a prescription for distinguishing true from false chirality, namely, the existence of an operator Q that is even(odd) under all chirality-preserving(chirality-flipping) symmetries of the crystal.

We then studied how to induce true chirality in materials with T_d symmetry. We introduced a parameter $Q'(\hat{B})$ to quantify the amount of chirality breaking. We applied this analysis to the specific case of InSb. There we showed, by exact diagonalization of a low-energy model, that for a magnetic field along low symmetry directions, the energies, velocities, and tilts are different for left- and right-handed Weyl cones. The differences in energy will lead to the quantized circular photogalvanic effect, while differences in tilt and velocities will lead to the chiral magnetic effect without external source of chirality and the helical magnetic effect.

For several directions and magnitudes of the magnetic field, the number of left- and right-handed type I cones (and number of left- and right-handed type II cones) are different. Of course, the total number of left- and right-handed cones remains equal, as required by topology. Since type I cones have a compact Fermi surface, and type II cones have a hyperbolic Fermi surface, this asymmetry between right- and left-handed Weyl cones of the same type will result in a highly nontrivial topology of Berry curvature.

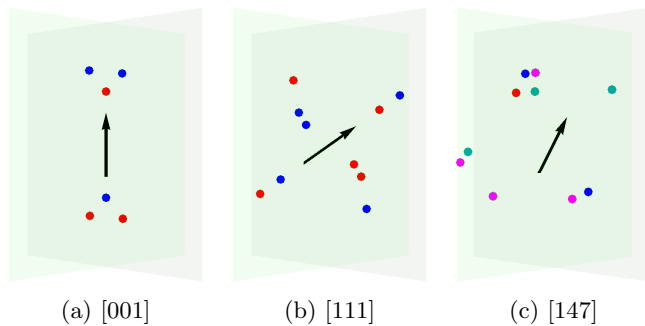


FIG. 3: Distribution of Weyl points in momentum space for a magnetic field of 0.75 T along high symmetry directions (a) [001] and (b) [111] and the low symmetry direction (c) [147]. The arrow denotes the direction of magnetic field. The color represents the chirality and type of the cones: red indicates left-handed type I, magenta indicates left-handed type II, blue indicates right-handed type I, and cyan indicates right-handed type II. For the low symmetry direction [147], there is no symmetry relating the cones.

Unlike intrinsically asymmetric Weyl materials, in the materials discussed in this manuscript, chirality-breaking effects are tunable, which may be desirable for measuring certain effects. Our results can be generalized to other space groups and different types of symmetry-breaking perturbations.

ACKNOWLEDGMENTS

We thank Dmitri Kharzeev, Gao Lanlan, and Mengkun Liu for useful and stimulating discussions. This work was supported in part by the U. S. Department of Energy under Awards DE-SC-0017662 (S. K.) and DE-FG02-88ER40388 (E. J. P.) and by the National Science Foundation under award DMR-1942447 (J. C.). J. C. acknowledges the support of the Flatiron Institute, a division of the Simons Foundation. J. C. and S. K. also acknowledge the support of an OVRP Seed Grant from Stony Brook University.

-
- [1] S. M. Young, S. Zaheer, J. C. Y. Teo, C. L. Kane, E. J. Mele, and A. M. Rappe, *Phys. Rev. Lett.* **108**, 140405 (2012).
- [2] Z. Wang, Y. Sun, X.-Q. Chen, C. Franchini, G. Xu, H. Weng, X. Dai, and Z. Fang, *Phys. Rev. B* **85**, 195320 (2012).
- [3] Z. Liu, B. Zhou, Y. Zhang, Z. Wang, H. Weng, D. Prabhakaran, S.-K. Mo, Z. Shen, Z. Fang, X. Dai, *et al.*, *Science* **343**, 864 (2014).
- [4] Z. Liu, J. Jiang, B. Zhou, Z. Wang, Y. Zhang, H. Weng, D. Prabhakaran, S. Mo, H. Peng, P. Dudin, *et al.*, *Nat. Mater.* **13**, 677 (2014).
- [5] J. A. Steinberg, S. M. Young, S. Zaheer, C. L. Kane, E. J. Mele, and A. M. Rappe, *Phys. Rev. Lett.* **112**, 036403 (2014).
- [6] B.-J. Yang and N. Nagaosa, *Nature Communications* **5**, 4898 (2014), [arXiv:1404.0754](https://arxiv.org/abs/1404.0754) [cond-mat.mes-hall].
- [7] B. Bradlyn, J. Cano, Z. Wang, M. Vergniory, C. Felser, R. Cava, and B. A. Bernevig, *Science* **353** (2016), [arXiv:1603.03093](https://arxiv.org/abs/1603.03093) [cond-mat.mes-hall].
- [8] J. Cano, B. Bradlyn, and M. G. Vergniory, *APL Materials* **7**, 101125 (2019), [arXiv:1904.12867](https://arxiv.org/abs/1904.12867) [cond-mat.mes-hall].
- [9] S. Klemenz, L. Schoop, and J. Cano, *Phys. Rev. B* **101**, 165121 (2020), [arXiv:1910.14036](https://arxiv.org/abs/1910.14036) [cond-mat.mes-hall].
- [10] B. J. Wieder, Z. Wang, J. Cano, X. Dai, L. M. Schoop, B. Bradlyn, and B. A. Bernevig, *Nature communications* **11**, 1 (2020).
- [11] X. Wan, A. M. Turner, A. Vishwanath, and S. Y. Savrasov, *Phys. Rev. B* **83**, 205101 (2011).
- [12] H. Weng, C. Fang, Z. Fang, B. A. Bernevig, and X. Dai, *Phys. Rev. X* **5**, 011029 (2015).
- [13] S.-M. Huang, S.-Y. Xu, I. Belopolski, C.-C. Lee, G. Chang, B. Wang, N. Alidoust, G. Bian, M. Neupane, C. Zhang, *et al.*, *Nat. Comm.* **6** (2015).
- [14] S.-Y. Xu, N. Alidoust, I. Belopolski, Z. Yuan, G. Bian, T.-R. Chang, H. Zheng, V. N. Strocov, D. S. Sanchez, G. Chang, C. Zhang, D. Mou, Y. Wu, L. Huang, C.-C. Lee, S.-M. Huang, B. Wang, A. Bansil, H.-T. Jeng, T. Neupert, A. Kaminski, H. Lin, S. Jia, and M. Zahid Hasan, *Nature Physics* **11**, 748 (2015), [arXiv:1504.01350](https://arxiv.org/abs/1504.01350) [cond-mat.mes-hall].
- [15] B. Q. Lv, N. Xu, H. M. Weng, J. Z. Ma, P. Richard, X. C. Huang, L. X. Zhao, G. F. Chen, C. E. Matt, F. Bisti, V. N. Strocov, J. Mesot, Z. Fang, X. Dai, T. Qian, M. Shi, and H. Ding, *Nature Physics* **11**, 724 (2015), [arXiv:1503.09188](https://arxiv.org/abs/1503.09188) [cond-mat.mtrl-sci].
- [16] S.-Y. Xu, I. Belopolski, N. Alidoust, M. Neupane, G. Bian, C. Zhang, R. Sankar, G. Chang, Z. Yuan, C.-C. Lee, S.-M. Huang, H. Zheng, J. Ma, D. S. Sanchez, B. Wang, A. Bansil, F. Chou, P. P. Shibayev, H. Lin, S. Jia, and M. Z. Hasan, *Science* **349**, 613 (2015), [arXiv:1502.03807](https://arxiv.org/abs/1502.03807) [cond-mat.mes-hall].
- [17] B. Q. Lv, H. M. Weng, B. B. Fu, X. P. Wang, H. Miao, J. Ma, P. Richard, X. C. Huang, L. X. Zhao, G. F. Chen, Z. Fang, X. Dai, T. Qian, and H. Ding, *Physical Review X* **5**, 031013 (2015), [arXiv:1502.04684](https://arxiv.org/abs/1502.04684) [cond-mat.mtrl-sci].
- [18] J. Xiong, S. K. Kushwaha, T. Liang, J. W. Krizan, M. Hirschberger, W. Wang, R. J. Cava, and N. P. Ong, *Science* **350**, 413 (2015).
- [19] N. P. Armitage, E. J. Mele, and A. Vishwanath, *Reviews of Modern Physics* **90**, 015001 (2018), [arXiv:1705.01111](https://arxiv.org/abs/1705.01111) [cond-mat.str-el].
- [20] K. Fukushima, D. E. Kharzeev, and H. J. Warringa, *Phys. Rev. D* **78**, 074033 (2008), [arXiv:0808.3382](https://arxiv.org/abs/0808.3382) [hep-ph].
- [21] V. Aji, *Phys. Rev. B* **85**, 241101 (2012), [arXiv:1108.4426](https://arxiv.org/abs/1108.4426) [cond-mat.str-el].
- [22] D. T. Son and B. Z. Spivak, *Phys. Rev. B* **88**, 104412 (2013), [arXiv:1206.1627](https://arxiv.org/abs/1206.1627) [cond-mat.mes-hall].
- [23] A. A. Burkov, *Phys. Rev. Lett.* **113**, 247203 (2014),

- arXiv:1409.0013 [cond-mat.mes-hall].
- [24] Q. Li, D. E. Kharzeev, C. Zhang, Y. Huang, I. Pletikosić, A. V. Fedorov, R. D. Zhong, J. A. Schneeloch, G. D. Gu, and T. Valla, *Nature Physics* **12**, 550 (2016), arXiv:1412.6543 [cond-mat.str-el].
- [25] X. Huang, L. Zhao, Y. Long, P. Wang, D. Chen, Z. Yang, H. Liang, M. Xue, H. Weng, Z. Fang, X. Dai, and G. Chen, *Physical Review X* **5**, 031023 (2015), arXiv:1503.01304 [cond-mat.mtrl-sci].
- [26] C.-L. Zhang, S.-Y. Xu, I. Belopolski, Z. Yuan, Z. Lin, B. Tong, G. Bian, N. Alidoust, C.-C. Lee, S.-M. Huang, T.-R. Chang, G. Chang, C.-H. Hsu, H.-T. Jeng, M. Neupane, D. S. Sanchez, H. Zheng, J. Wang, H. Lin, C. Zhang, H.-Z. Lu, S.-Q. Shen, T. Neupert, M. Zahid Hasan, and S. Jia, *Nature Communications* **7**, 10735 (2016), arXiv:1601.04208 [cond-mat.mtrl-sci].
- [27] Z. Wang, Y. Zheng, Z. Shen, Y. Lu, H. Fang, F. Sheng, Y. Zhou, X. Yang, Y. Li, C. Feng, and Z.-A. Xu, *Phys. Rev. B* **93**, 121112 (2016), arXiv:1506.00924 [cond-mat.mes-hall].
- [28] F. Arnold, C. Shekhar, S.-C. Wu, Y. Sun, R. D. Dos Reis, N. Kumar, M. Naumann, M. O. Ajeesh, M. Schmidt, A. G. Grushin, J. H. Bardarson, M. Baenitz, D. Sokolov, H. Borrmann, M. Nicklas, C. Felser, E. Hassinger, and B. Yan, *Nature Communications* **7**, 11615 (2016), arXiv:1506.06577 [cond-mat.mtrl-sci].
- [29] C.-K. Chan, N. H. Lindner, G. Refael, and P. A. Lee, *Phys. Rev. B* **95**, 041104 (2017), arXiv:1607.07839 [cond-mat.mes-hall].
- [30] Q. Ma, S.-Y. Xu, C.-K. Chan, C.-L. Zhang, G. Chang, Y. Lin, W. Xie, T. Palacios, H. Lin, S. Jia, P. A. Lee, P. Jarillo-Herrero, and N. Gedik, *Nature Physics* **13**, 842 (2017), arXiv:1705.00590 [cond-mat.mtrl-sci].
- [31] Y. Gao, S. Kaushik, E. J. Philip, Z. Li, Y. Qin, Y. P. Liu, W. L. Zhang, Y. L. Su, X. Chen, H. Weng, D. E. Kharzeev, M. K. Liu, and J. Qi, *Nature Communications* **11**, 720 (2020), arXiv:1901.00986 [cond-mat.mtrl-sci].
- [32] F. de Juan, A. G. Grushin, T. Morimoto, and J. E. Moore, *Nature Communications* **8**, 15995 (2017), arXiv:1611.05887 [cond-mat.str-el].
- [33] D. E. Kharzeev, Y. Kikuchi, R. Meyer, and Y. Tanizaki, *Phys. Rev. B* **98**, 014305 (2018), arXiv:1801.10283 [cond-mat.mes-hall].
- [34] D. E. Kharzeev, Y. Kikuchi, and R. Meyer, *European Physical Journal B* **91**, 83 (2018), arXiv:1610.08986 [cond-mat.mes-hall].
- [35] G. Chang, S.-Y. Xu, B. J. Wieder, D. S. Sanchez, S.-M. Huang, I. Belopolski, T.-R. Chang, S. Zhang, A. Bansil, H. Lin, and M. Z. Hasan, *Phys. Rev. Lett.* **119**, 206401 (2017).
- [36] Z. Rao, H. Li, T. Zhang, S. Tian, C. Li, B. Fu, C. Tang, L. Wang, Z. Li, W. Fan, J. Li, Y. Huang, Z. Liu, Y. Long, C. Fang, H. Weng, Y. Shi, H. Lei, Y. Sun, T. Qian, and H. Ding, *Nature (London)* **567**, 496 (2019).
- [37] D. Rees, K. Manna, B. Lu, T. Morimoto, H. Borrmann, C. Felser, J. E. Moore, D. H. Torchinsky, and J. Orenstein, *Science Advances* **6**, eaba0509 (2020), arXiv:1902.03230 [cond-mat.mes-hall].
- [38] Z. Ni, K. Wang, Y. Zhang, O. Pozo, B. Xu, X. Han, K. Manna, J. Paglione, C. Felser, A. G. Grushin, F. de Juan, E. J. Mele, and L. Wu, (2020), arXiv:2006.09612 [cond-mat.mtrl-sci].
- [39] A. A. Soluyanov, D. Gresch, Z. Wang, Q. Wu, M. Troyer, X. Dai, and B. A. Bernevig, *Nature (London)* **527**, 495 (2015), arXiv:1507.01603 [cond-mat.mes-hall].
- [40] L. X. Yang, Z. K. Liu, Y. Sun, H. Peng, H. F. Yang, T. Zhang, B. Zhou, Y. Zhang, Y. F. Guo, M. Rahn, D. Prabhakaran, Z. Hussain, S. K. Mo, C. Felser, B. Yan, and Y. L. Chen, *Nature Physics* **11**, 728 (2015).
- [41] P. Li, Y. Wen, X. He, Q. Zhang, C. Xia, Z.-M. Yu, S. A. Yang, Z. Zhu, H. N. Alshareef, and X.-X. Zhang, *Nature Communications* **8**, 2150 (2017).
- [42] M. Zhang, Z. Yang, and G. Wang, *The Journal of Physical Chemistry C* **122**, 3533 (2018).
- [43] L. D. Barron, *Journal of the American Chemical Society* **108**, 5539 (1986).
- [44] N. Xu, H. M. Weng, B. Q. Lv, C. E. Matt, J. Park, F. Bisti, V. N. Strocov, D. Gawryluk, E. Pomjakushina, K. Conder, N. C. Plumb, M. Radovic, G. Autès, O. V. Yazyev, Z. Fang, X. Dai, T. Qian, J. Mesot, H. Ding, and M. Shi, *Nature Communications* **7**, 11006 (2016), arXiv:1507.03983 [cond-mat.mtrl-sci].
- [45] K. A. Modic, T. Meng, F. Ronning, E. D. Bauer, P. J. W. Moll, and B. J. Ramshaw, *Scientific Reports* **9**, 2095 (2019).
- [46] X. Yuan, C. Zhang, Y. Zhang, Z. Yan, T. Lyu, M. Zhang, Z. Li, C. Song, M. Zhao, P. Leng, M. Ozerov, X. Chen, N. Wang, Y. Shi, H. Yan, and F. Xiu, *Nature Communications* **11**, 1259 (2020).
- [47] S. Sun, Z. Song, H. Weng, and X. Dai, *Phys. Rev. B* **101**, 125118 (2020), arXiv:1910.01378 [cond-mat.mes-hall].
- [48] M. Hirschberger, S. Kushwaha, Z. Wang, Q. Gibson, S. Liang, C. A. Belvin, B. A. Bernevig, R. J. Cava, and N. P. Ong, *Nature Materials* **15**, 1161 (2016), arXiv:1602.07219 [cond-mat.str-el].
- [49] J. Cano, B. Bradlyn, Z. Wang, M. Hirschberger, N. P. Ong, and B. A. Bernevig, *Phys. Rev. B* **95**, 161306 (2017), arXiv:1604.08601 [cond-mat.mes-hall].
- [50] J. Ruan, S.-K. Jian, H. Yao, H. Zhang, S.-C. Zhang, and D. Xing, *Nature Communications* **7**, 11136 (2016), arXiv:1511.08284 [cond-mat.mes-hall].
- [51] C. Shekhar, N. Kumar, V. Grinenko, S. Singh, R. Sarkar, H. Luetkens, S.-C. Wu, Y. Zhang, A. C. Komarek, E. Kampert, Y. Skourski, J. Wosnitza, W. Schnelle, A. McCollam, U. Zeitler, J. Kübler, B. Yan, H. H. Klauss, S. S. P. Parkin, and C. Felser, *Proceedings of the National Academy of Science* **115**, 9140 (2018), arXiv:1604.01641 [cond-mat.mtrl-sci].
- [52] F. Qu, J. van Veen, F. K. de Vries, A. J. A. Beukman, M. Wimmer, W. Yi, A. A. Kiselev, B.-M. Nguyen, M. Sokolich, M. J. Manfra, F. Nichele, C. M. Marcus, and L. P. Kouwenhoven, *Nano Letters* **16**, 7509 (2016), arXiv:1608.05478 [cond-mat.mes-hall].
- [53] H. A. Nilsson, P. Caroff, C. Thelander, M. Larsson, J. B. Wagner, L.-E. Wernersson, L. Samuelson, and H. Q. Xu, *Nano Letters* **9**, 3151 (2009).
- [54] I. Vurgaftman, J. R. Meyer, and L. R. Ram-Mohan, *Journal of Applied Physics* **89**, 5815 (2001).